

The persistent photoconductivity effect in AlGaN/GaN heterostructures grown on sapphire and SiC substrates

Engin Arslan,^{1,a)} Serkan Bütün,¹ S. Bora Lisesivdin,² Mehmet Kasap,² Suleyman Ozcelik,² and Ekmel Ozbay¹

¹*Department of Physics, Department of Electrical and Electronics Engineering, Nanotechnology Research Center-NANOTAM, Bilkent University, 06800 Ankara, Turkey*

²*Department of Physics, Faculty of Science and Arts, Gazi University, Teknikokullar, 06500 Ankara, Turkey*

(Received 24 September 2007; accepted 12 March 2008; published online 16 May 2008)

In the present study, we reported the results of the investigation of electrical and optical measurements in $\text{Al}_x\text{Ga}_{1-x}\text{N}/\text{GaN}$ heterostructures ($x=0.20$) that were grown by way of metal-organic chemical vapor deposition on sapphire and SiC substrates with the same buffer structures and similar conditions. We investigated the substrate material effects on the electrical and optical properties of $\text{Al}_{0.20}\text{Ga}_{0.80}\text{N}/\text{GaN}$ heterostructures. The related electrical and optical properties of $\text{Al}_x\text{Ga}_{1-x}\text{N}/\text{GaN}$ heterostructures were investigated by variable-temperature Hall effect measurements, photoluminescence (PL), photocurrent, and persistent photoconductivity (PPC) that in turn illuminated the samples with a blue ($\lambda=470$ nm) light-emitting diode (LED) and thereby induced a persistent increase in the carrier density and two-dimensional electron gas (2DEG) electron mobility. In sample A ($\text{Al}_{0.20}\text{Ga}_{0.80}\text{N}/\text{GaN}/\text{sapphire}$), the carrier density increased from 7.59×10^{12} to 9.9×10^{12} cm^{-2} via illumination at 30 K. On the other hand, in sample B ($\text{Al}_{0.20}\text{Ga}_{0.80}\text{N}/\text{GaN}/\text{SiC}$), the increments in the carrier density were larger than those in sample A, in which it increased from 7.62×10^{12} to 1.23×10^{13} cm^{-2} at the same temperature. The 2DEG mobility increased from 1.22×10^4 to 1.37×10^4 $\text{cm}^{-2}/\text{V s}$ for samples A and B, in which 2DEG mobility increments occurred from 3.83×10^3 to 5.47×10^3 $\text{cm}^{-2}/\text{V s}$ at 30 K. The PL results show that the samples possessed a strong near-band-edge exciton luminescence line at around 3.44 and 3.43 eV for samples A and B, respectively. The samples showed a broad yellow band spreading from 1.80 to 2.60 eV with a peak maximum at 2.25 eV with a ratio of a near-band-edge excitation peak intensity up to a deep-level emission peak intensity ratio that were equal to 3 and 1.8 for samples A and B, respectively. Both of the samples that were illuminated with three different energy photon PPC decay behaviors can be well described by a stretched-exponential function and relaxation time constant τ as well as a decay exponent β that changes with the substrate type. The energy barrier for the capture of electrons in the 2DEG channel via the deep-level impurities (DX-like centers) in AlGaN for the $\text{Al}_{0.20}\text{Ga}_{0.80}\text{N}/\text{GaN}/\text{sapphire}$ and $\text{Al}_{0.20}\text{Ga}_{0.80}\text{N}/\text{GaN}/\text{SiC}$ heterojunction samples are 343 and 228 meV, respectively. The activation energy for the thermal capture of an electron by the defects ΔE changed with the substrate materials. Our results show that the substrate material strongly affects the electrical and optical properties of $\text{Al}_{0.20}\text{Ga}_{0.80}\text{N}/\text{GaN}$ heterostructures. These results can be explained with the differing degrees of the lattice mismatch between the grown layers and substrates. © 2008 American Institute of Physics. [DOI: 10.1063/1.2921832]

I. INTRODUCTION

The transport properties of GaN and its alloys are attracting increasing interest due to the potential application of these materials for solar blind photodetectors and high mobility transistors.¹⁻⁴ Because of the large band gap, the applications of $\text{Al}_x\text{Ga}_{1-x}\text{N}$ are extensive, such as for visible-blind ultraviolet detectors, laser diodes, and short-wave light-emitting diodes (LEDs).^{5,6} High-quality AlGaN/GaN heterostructures have been shown to contain two-dimensional electron gas (2DEG), which has attracted special interest due to its potential applications in high mobility transistors operating at high power and high temperature levels.⁷⁻¹⁰

The device structures are usually grown on highly lattice-mismatched substrates, such as sapphire,¹¹ SiC,¹² or

Si.¹³ It still remains difficult to obtain a high-quality GaN epilayer because of the large lattice mismatch ($\sim 14\%$ for sapphire and $\sim 3.5\%$ for SiC) as well as the difference in the thermal expansion coefficients ($\sim 80\%$ for sapphire and $\sim 3.2\%$ for SiC) between the GaN film and sapphire and SiC substrates. This significant difference between the lattice parameters, as well as the thermal expansion coefficients between the film and substrate, results in a high level of in-plane stress and threading dislocation density generation, as grown by metal-organic chemical vapor deposition (MOCVD) in the GaN epitaxial layer.¹¹⁻¹³ These dislocations affect the performance of several devices.^{1,2} The effects of lattice and thermal mismatching between GaN films and substrates, such as sapphire (Al_2O_3),¹² SiC,¹² and Si,¹³ have led to extensive further research.

The persistent photoconductivity (PPC) effect is a light-

^{a)}Electronic mail: engina@bilkent.edu.tr.

induced enhancement in the conductivity that persists for a long period after the termination of light excitation.^{14,15} This interesting phenomenon has been observed in many II-VI (Ref. 16) and III-V (Refs. 17 and 18) semiconductors, including the *p*- and *n*-type GaN epilayers,¹⁹ Si or Se doped *n*-type GaN,^{2,20} or Mg doped GaN,^{20,21} AlGaN/GaN heterostructures,^{22–25} and AlGaN epilayers.^{25,26} Other related studies are rather useful for understanding the metastable properties of defects, the mechanisms for carrier storage and relaxation, and the transport properties in a disordered system.^{16–18,27,28}

The increments in the carrier concentration are due to the photoexcited electrons that are transferred from the deep-level donors (e.g., DX centers in $\text{Al}_x\text{Ga}_{1-x}\text{As}$) to the conduction band when the light is turned on. If the incident light is turned off at a low temperature, the recombination of the electrons and ionized deep-level donors can be prevented by the local potential barrier around the deep-level donors.²⁹ This results in a persistent carrier concentration, which can be used to obtain a PPC under an applied voltage bias.³⁰ The PPC effect in $\text{Al}_x\text{Ga}_{1-x}\text{As}$ is induced by the metastable DX centers.²⁹ However, in the heterostructure and quantum well structures, the PPC effect is no longer limited to the presence of DX centers. The other deep-level donors in the heterostructures are able to produce a PPC effect as long as the deep donor level is below the Fermi energy.^{21,30} In the GaN and $\text{Al}_x\text{Ga}_{1-x}\text{N}$ epilayers, this was similarly ascribed to defect complexes such as gallium vacancies, nitrogen antisites, deep-level impurities, and interacting defect complexes.^{19,20,28,29,31–34} In the literature, several studies can be found about PPC experiments on $\text{Al}_x\text{Ga}_{1-x}\text{N}/\text{GaN}$ heterostructures.^{22–25} In those studies, the persistent increase in the carrier concentration was explained by the transfer of photoexcited electrons from the deep-level impurities in the $\text{Al}_x\text{Ga}_{1-x}\text{N}$ layers.²⁴

In the present work, we investigated the substrate material effects on the electrical and optical properties of $\text{Al}_{0.20}\text{Ga}_{0.80}\text{N}/\text{GaN}$ heterostructures by Hall measurements, using photoluminescence (PL), photocurrent (PC), and PPC measurements. The results of the 2DEG carrier mobilities and carrier concentration behavior in a dark state and under the PPC state, PL, PC, and PPC in the AlGaN/GaN heterojunction are given. The deep-level defect properties, which are related to yellow band (YB) and PPC, are also discussed. Two different substrate structures were used in the present study. AlGaN/GaN heterojunctions were grown on sapphire and SiC substrates with the same growth conditions and buffer structures. The results reveal that the lattice relaxation of the DX-like impurity centers is responsible for the observed PPC in AlGaN/GaN ($x=0.20$) heterostructures. The activation energy (electron-capture barrier), which is required to return the photoexcited electrons from the shallow state to the DX-like deep state, was found to change with the substrate materials.

II. EXPERIMENTAL PROCEDURE

The $\text{Al}_x\text{Ga}_{1-x}\text{N}/\text{GaN}$ ($x=0.20$) heterostructures on (0001) on a double-polished 2 in. (0001) sapphire (Al_2O_3)

and 6H-SiC substrates were grown in a low pressure MOCVD reactor (Aixtron 200/4 HT-S), using trimethylgallium, trimethylaluminum, and ammonia as Ga, Al, and N precursors, respectively. The buffer structures consisted of a 15 nm thick, low temperature (650 °C) AlN nucleation layer and a high temperature (1150 °C) 0.5 nm AlN template. A 2 μm nominally undoped GaN layer was grown on an AlN template layer at 1050 °C, followed by a 1 nm thick high temperature AlN (1150 °C) barrier layer.

The AlN barrier layer was used to reduce the alloy disorder scattering by minimizing the wave function penetration from the two-dimensional electron gas (2DEG) channel into the $\text{Al}_x\text{Ga}_{1-x}\text{N}$ layer.^{35,36} After the deposition of these layers, a 20 nm thick undoped $\text{Al}_{0.20}\text{Ga}_{0.80}\text{N}$ layer was grown on an AlN barrier layer at 1050 °C and, finally, a 3 nm GaN cap layer was grown at the same temperature. At the beginning of the growth, the substrate was baked in H_2 ambient conditions at 1100 °C for 5 min in order to remove the native oxide. $\text{Al}_x\text{Ga}_{1-x}\text{N}/\text{GaN}$ ($x=0.20$) heterostructures were grown on 6H-SiC substrate with the same structures and similar growth conditions. Hereinafter, we will call the $\text{Al}_{0.20}\text{Ga}_{0.80}\text{N}/\text{GaN}/\text{sapphire}$ and $\text{Al}_{0.20}\text{Ga}_{0.80}\text{N}/\text{GaN}/\text{SiC}$ heterojunctions as sample A and sample B, respectively.

PL measurements were performed at room temperature. PL spectra were excited using a He–Cd laser (325 nm) with an excitation power of 15 mW. For the PC and PPC measurements, the samples were cut into $4 \times 4 \text{ mm}^2$, in which four contacts at the corners of the sample were formed with Ti/Al/Ni/Au solder. The Ohmic nature of the contacts was confirmed by the *I*-*V* characteristics. For the PPC measurements, a constant direct 2 V bias voltage was supplied to the sample and the conductivity was then measured by a Keithley 236 source measure unit. For the sample, an illumination Xe lamp was used as the photoexcitation light source, which was dispersed by a monochromator. The 2DEG electron density and mobility were determined by variable-temperature Hall measurements between 30 and 300 K at a magnetic field of 0.5 T. For the PPC effect measurements, the samples were illuminated with a blue ($\lambda=470 \text{ nm}$) LED. The PC spectra were recorded for various photon energies of incident light between 2.20 and 4.90 eV and the PPC measurements were performed for three different photon energies: 2.06, 2.95, and 3.70 eV. We used illumination light that had the same intensity. Before the light illumination, the samples were kept in the dark for 24 h in order to accurately determine the dark current.

III. RESULTS AND DISCUSSION

The 2DEG carrier mobilities and carrier concentration behavior for samples A and B were measured in the dark as well as under illumination at different temperatures. The results are shown in Figs. 1(a) and 1(b). The data for all of the curves shown in Fig. 1 were collected in the dark. The initial data were collected before the sample was illuminated. Subsequently, we exposed the sample to light for 10 min with photon energies of 2.64 eV from the LED. The LED was then turned off and the sample was allowed to stabilize.

The carrier density and mobility were relatively insensi-

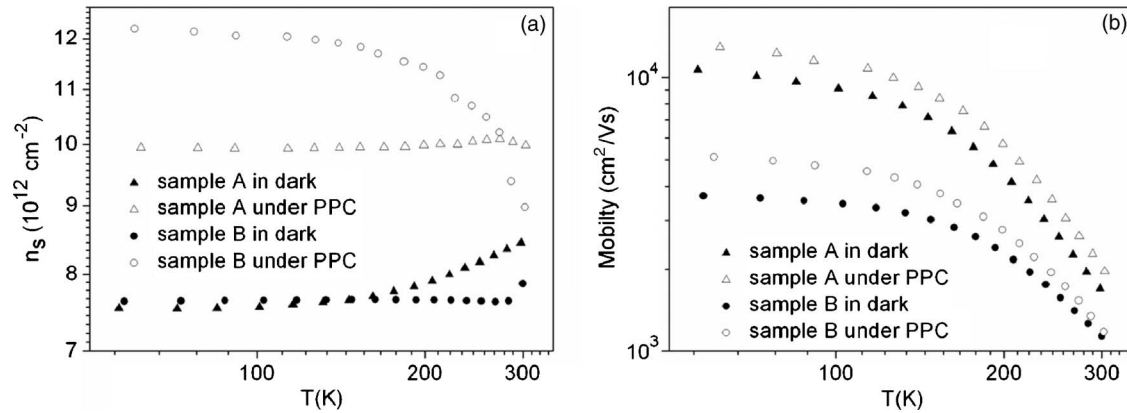


FIG. 1. The measured (a) 2DEG carrier density n_s and (b) mobility μ in $\text{Al}_{0.20}\text{Ga}_{0.80}\text{N}/\text{GaN}/\text{sapphire}$ and $\text{Al}_{0.20}\text{Ga}_{0.80}\text{N}/\text{GaN}/\text{SiC}$ heterostructures as a function of temperature T measured in the dark state and in the PPC state.

tive to the temperature at low temperature values. This behavior is typical for the 2DEG. Similar results were observed previously for 2DEG systems in $\text{AlGaAs}/\text{GaAs}$ (Ref. 29) and $\text{AlGaIn}/\text{GaIn}$ heterojunctions^{24,34} in the dark state as well as under illumination. The 2DEG mobility and carrier concentration were enhanced significantly for all of the temperatures after photoexcitation.¹⁰

Figure 1(a) shows that the illumination resulted in an increase in the carrier density at all of the temperatures used for both samples. In sample A, the carrier density increased from 7.59×10^{12} to $9.93 \times 10^{12} \text{ cm}^{-2}$ by way of illumination at 30 K, but in sample B, the increments in the carrier density were larger than those in sample A, in which it increased from 7.62×10^{12} to $1.23 \times 10^{13} \text{ cm}^{-2}$ at the same temperature.

This increment in the carrier density is in agreement with recent PPC reports from other authors.^{10,24,29} The difference between the increments ratio in both samples comes from the DX center density in the AlGaIn layers. The 2DEG mobility increment ratios, due to photoexcitation at a fixed temperature, are different for samples A and B. In fact, at 30 K, it increased from 1.22×10^4 to $1.37 \times 10^4 \text{ cm}^2/\text{Vs}$ for sample A. On the other hand, in sample B, the 2DEG mobility increments occur from 3.83×10^3 to $5.47 \times 10^3 \text{ cm}^2/\text{Vs}$ at the same temperature.

One of the dominant scattering mechanisms that limit the mobility of a 2DEG is remote ionized impurity scattering.^{7-9,29,35,36} The increments in mobility due to photoexcitation at a fixed temperature can be attributed to the increased electron mean energy with an increasing carrier density in the 2DEG channel, which leads to an improved screening and thereby reduced scattering between the 2DEG electrons with the ionized donor impurities.^{24,29}

The PL measurements taken for the $\text{Al}_{0.20}\text{Ga}_{0.80}\text{N}/\text{GaN}/\text{sapphire}$ and $\text{Al}_{0.20}\text{Ga}_{0.80}\text{N}/\text{GaN}/\text{SiC}$ samples at room temperature are shown in Fig. 2. As seen in Fig. 2, the samples show a strong near-band-edge exciton luminescence line around 3.44 and 3.43 eV for samples A and B, respectively. The full widths at half maximum of 30 meV for sample A and 35 meV for sample B are comparable to that of the high-quality GaN. The energy position of the excitonic PL band is shifted by ~ 10 meV for $\text{Al}_{0.20}\text{Ga}_{0.80}\text{N}/\text{GaN}/$

sapphire and ~ 20 meV for $\text{Al}_{0.20}\text{Ga}_{0.80}\text{N}/\text{GaN}/\text{SiC}$ toward high energies compared to the position of the respective excitons in the nonstressed GaN layers.⁹ These results show that there are considerable compressive strains that exist in our GaN layers due to the mismatch between the epilayers. In our case, the compressive strains in GaN on sapphire are larger than those in GaN on SiC.^{11,13}

In addition, the broad deep-level emission centered at approximately 2.2 eV that is modulated by the Fabry-Pérot interference fringes was observed. The appearance of the interference indicates the smooth surface of the film. PL measurements performed on both samples showed a broad yellow PL spreading from 1.80 to 2.60 eV with a maximum peak at 2.25 eV. The YB PL emission is generally believed to result from nitrogen vacancies and from impurities such as oxygen.^{3,17,37} The ratio of the near-band-edge excitation peak intensity to the deep-level emission peak intensity ratio is equal to 3 and 1.8 for samples $\text{Al}_{0.20}\text{Ga}_{0.80}\text{N}/\text{GaN}/\text{sapphire}$ and $\text{Al}_{0.20}\text{Ga}_{0.80}\text{N}/\text{GaN}/\text{SiC}$, respectively. This result shows that the $\text{Al}_{0.20}\text{Ga}_{0.80}\text{N}/\text{GaN}/\text{SiC}$ sample contains more defect density than the $\text{Al}_{0.20}\text{Ga}_{0.80}\text{N}/\text{GaN}/\text{sapphire}$ sample. Broad peaks were observed between 2.65 and 3.25 eV for both samples. These peaks may be related to the acceptor levels.

To investigate the energy distribution of the trap levels,

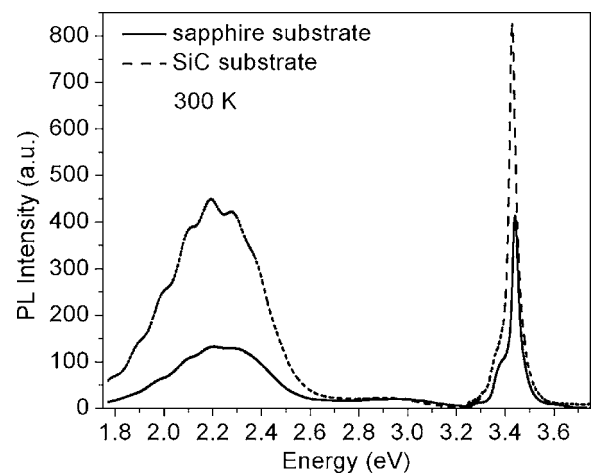


FIG. 2. Room temperature PL spectra of $\text{Al}_{0.20}\text{Ga}_{0.80}\text{N}/\text{GaN}/\text{sapphire}$ and $\text{Al}_{0.20}\text{Ga}_{0.80}\text{N}/\text{GaN}/\text{SiC}$ heterostructure samples.

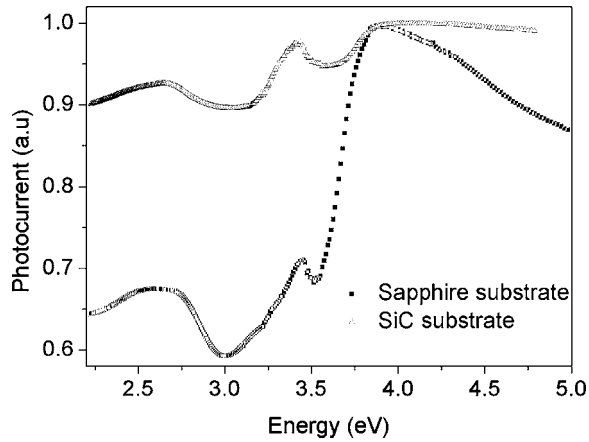


FIG. 3. Photoconductivity spectrum of $\text{Al}_{0.20}\text{Ga}_{0.80}\text{N}/\text{GaN}/\text{sapphire}$ and $\text{Al}_{0.20}\text{Ga}_{0.80}\text{N}/\text{GaN}/\text{SiC}$ heterostructure samples taken at room temperature.

PC spectra were measured for those excitation energies ranging from 2.20 to 4.90 eV. Figure 3 shows the resulting PC spectrum of the $\text{Al}_{0.20}\text{Ga}_{0.80}\text{N}/\text{GaN}$ heterojunction on sapphire and on SiC substrate at room temperature. The PC spectrum of both samples exhibited three peaks at the energies of 3.83, 3.44, and 2.60 eV for sample A and 3.83, 3.43, and 2.60 eV for sample B, which correspond to the band gaps of AlGaN and GaN as well as the GaN YB, respectively. In Fig. 3, the increments in the PC peak intensity of the AlGaN epilayer as a greater number of incident photons were shown. Because the photon hits the surface without any loss and generates a greater number of electron-hole pairs, the light intensity absorbed at the GaN layer is decreased, resulting in low-intensity band-edge and YB peaks. This resulted in good agreement with the previous published results.²³

When the $\text{Al}_{0.20}\text{Ga}_{0.80}\text{N}/\text{GaN}$ heterojunction samples were illuminated with the photon energies of 2.06, 2.95, and 3.70 eV, PPC was observed in both heterojunctions that were grown on sapphire and SiC substrates. The PPC decay curve samples were normalized to unity at $t=0$ according to $I_{\text{ppc}}(t)=[I(t)-I_d]/[I(0)-I_d]$, where $I(0)$ is defined as the current immediately after the termination of the excitation, $I(t)$ as the current at decay time t , and I_d as the initial dark current (Fig. 4). The inset in Fig. 4 shows the PC as a function

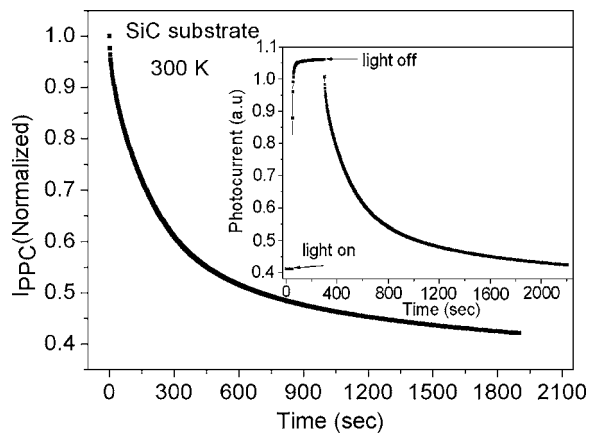


FIG. 4. Room temperature PPC decay kinetics of the $\text{Al}_{0.20}\text{Ga}_{0.80}\text{N}/\text{GaN}/\text{SiC}$ heterostructure.

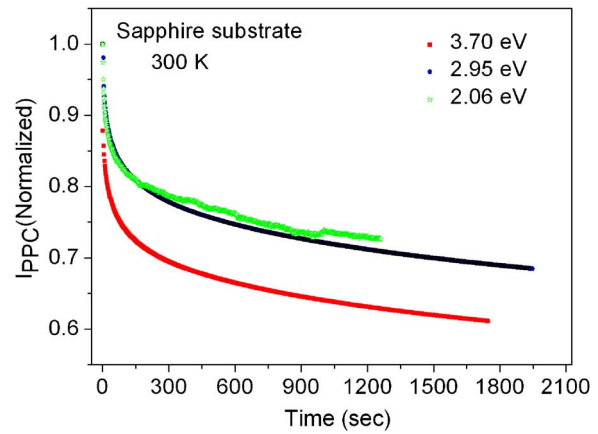


FIG. 5. (Color online) Room temperature PPC decay kinetics of the $\text{Al}_{0.20}\text{Ga}_{0.80}\text{N}/\text{GaN}/\text{sapphire}$ heterostructure as a function of excitation energy.

of time and illumination in the $\text{Al}_{0.20}\text{Ga}_{0.80}\text{N}/\text{GaN}/\text{SiC}$ heterojunction.

Figure 5 shows the PPC spectra of sample A as a function of excitation photon energy at 300 K. Both of the samples exhibited an initial fast decrease that was then followed by a slower, but steady, decrement. The rate of the PC decrements changes with the photon energy. Such PPC behavior has been observed in many III-V and II-VI semiconductor thin films and heterostructures.^{19-26,28,30-32,38-41} The origin of the PPC can be explained by the fact that the photoexcited carriers are trapped and spatially separated by local potential fluctuations, which then suppresses the recombination of carriers. The Al content affects the PPC decay rate. Decreasing the Al content causes a faster decay. The carrier transport process can be used for interpreting the slow decay in those samples with high Al compositions. The carrier capture process, from weakly localized states to strongly localized states of deeper potential by alloy fluctuations, causes a slow decay in PPC.^{19,22} In addition, the stretched-exponential relaxation is commonly observed in disordered samples.^{24,31}

The persistent increase in the conductivity in the 2DEG channel after the illumination of the PPC in AlGaN/GaN heterostructures can be explained via three possible mechanisms. One such mechanism is the photoionization of deep-level donors in the AlGaN barrier. The second is the photoionization of deep-level donors in the GaN layer. The last is the electron-hole pair generation in the GaN layer with a subsequent charge separation by the electric field from the macroscopic barrier due to band bending. In order to identify the main mechanism for PPC, we used three different photon energy levels (2.06, 2.95, and 3.70 eV) as illumination sources. Under the excitation with the photon energy conditions of $\hbar\nu < E_g$ (2.06 and 2.95 eV) of GaN, the energy of the excitation photons was insufficiently large to generate electron-hole pairs in the GaN layer. For the case of $\hbar\nu < E_g$ (3.70 eV) of GaN, in addition to the photoexcitation of deep-level impurities, band-to-band excitation also generates electron-hole pairs in the GaN layer.

In order to determine the origin of the PPC in $\text{Al}_{0.20}\text{Ga}_{0.80}\text{N}/\text{GaN}$ heterostructures, we also performed comparison measurements on the GaN epilayers. For these

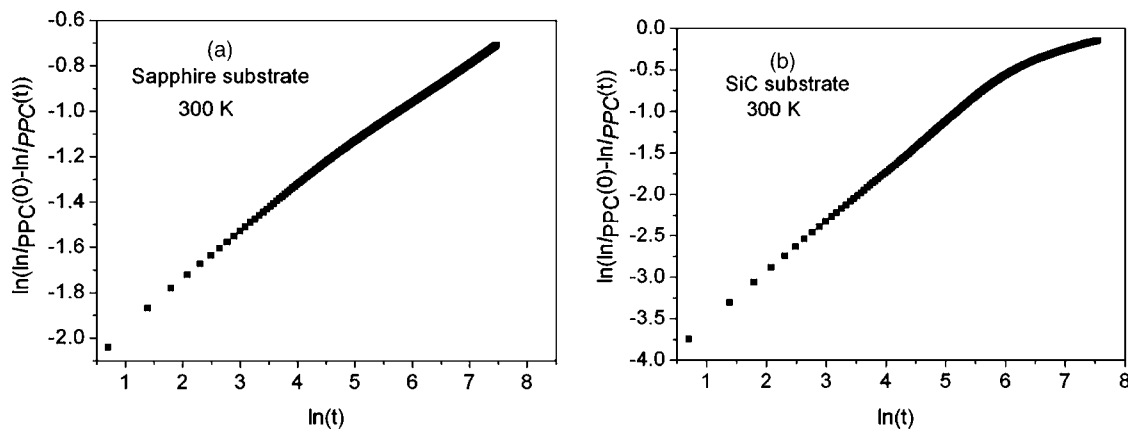


FIG. 6. Plot of $\ln[\ln I_{\text{PPC}}(0) - \ln I_{\text{PPC}}(t)]$ vs $\ln(t)$ for (a) $\text{Al}_{0.20}\text{Ga}_{0.80}\text{N}/\text{GaN}/\text{sapphire}$ and (b) $\text{Al}_{0.20}\text{Ga}_{0.80}\text{N}/\text{GaN}/\text{SiC}$ heterostructures at room temperature. The linear curves indicate that PPC decays according to stretched-exponential function.

measurements, the AlGaN/AlN layers were etched from the $\text{Al}_{0.20}\text{Ga}_{0.80}\text{N}/\text{GaN}/\text{sapphire}$ and $\text{Al}_{0.20}\text{Ga}_{0.80}\text{N}/\text{GaN}/\text{SiC}$ heterojunction samples, in which the PPC effect was absent in the GaN epilayers. In this case, the second mechanism can be precluded for our $\text{Al}_{0.20}\text{Ga}_{0.80}\text{N}/\text{GaN}$ heterostructures. These results suggest that the carrier density in the 2DEG channel is primarily contributed by the transfer of photoexcited electrons from the deep-level impurities (or DX centers) in the $\text{Al}_x\text{Ga}_{1-x}\text{N}/\text{AlN}$ barrier layer.²⁹ Because of the thin AlN interfacial layer, deep-level impurities in the $\text{Al}_x\text{Ga}_{1-x}\text{N}$ layer may be responsible for the PPC response. These deep levels can be compared to the DX centers in the $\text{Al}_x\text{Ga}_{1-x}\text{As}$ layers.¹⁷

The decay kinetics in PC after turning off the illumination can be described well by a stretched-exponential function,³⁷

$$I_{\text{PPC}}(t) = I_{\text{PPC}}(0) \exp[-(t/\tau)^\beta] \quad (0 < \beta < 1), \quad (1)$$

where $I_{\text{PPC}}(0)$ is the initial PC value, τ is the PPC decay time constant, and β is the decay exponent. This was demonstrated by plotting $\ln[\ln I_{\text{PPC}}(0) - \ln I_{\text{PPC}}(t)]$ versus $\ln(t)$ for the PPC decay curves. Figures 6(a) and 6(b) show a representative plot of $\ln[\ln I_{\text{PPC}}(0) - \ln I(t)]$ versus $\ln(t)$ for samples A and B at 300 K. The solid line is the least-squares fit of data with Eq. (1) for the PPC decay. The good linear

behavior that was observed is shown in Fig. 5. The linear behavior of the plot demonstrates that PPC decay can be described well by Eq. (1). The stretched-exponential relaxation is commonly observed in disordered systems,^{26,28,30,33,37,40,41} which implies that the origin of the observed PPC effect has a similar property. A least-squares fit to the experimental data yields a time constant τ and decay exponent β values.

The fitted parameters for the PPC decay were $\tau = 8.8 \times 10^4$ s, $\beta = 0.25$ for sample A and $\tau = 1.9 \times 10^3$ s, $\beta = 0.43$ for sample B at 300 K, respectively. The time constant (τ) and β that was found for $\text{Al}_{0.20}\text{Ga}_{0.80}\text{N}/\text{GaN}/\text{sapphire}$ are consistent with the values noted in the literature.^{24,34} However, the values found for $\text{Al}_{0.20}\text{Ga}_{0.80}\text{N}/\text{GaN}/\text{sapphire}$ heterostructures are larger than the given values. The difference between these values results from the compressive strain difference in the GaN layers due to the mismatch between the epilayers.

The temperature-dependence measurements of PPC were studied in order to further investigate the origin of the PPC effect phenomena in $\text{Al}_x\text{Ga}_{1-x}\text{N}/\text{GaN}$ heterostructures. As shown in Fig. 7, the PPC effect strongly depends on the temperature. The decay times of the PC depend on the temperature and become longer with a decreasing temperature.

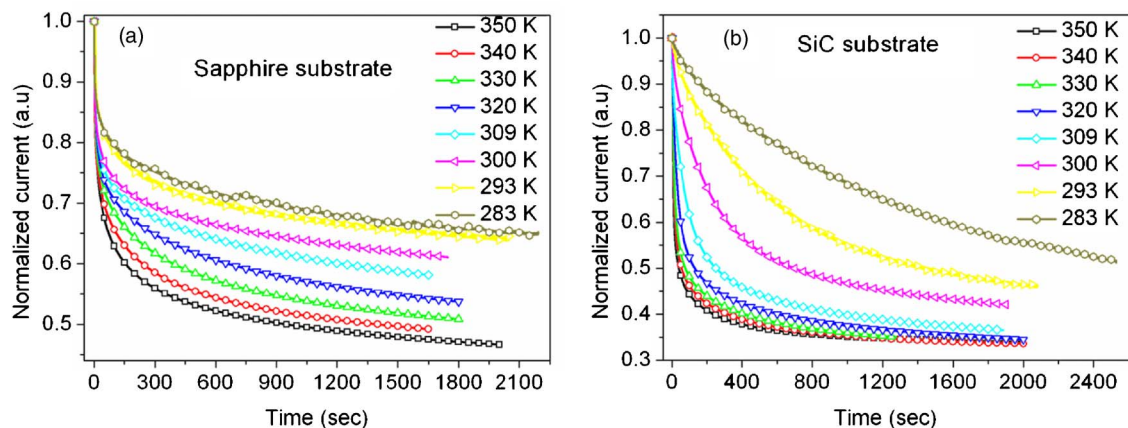


FIG. 7. (Color online) The PPC decay kinetics of (a) $\text{Al}_{0.20}\text{Ga}_{0.80}\text{N}/\text{GaN}/\text{sapphire}$ and (b) $\text{Al}_{0.20}\text{Ga}_{0.80}\text{N}/\text{GaN}/\text{SiC}$ heterostructures as a function of temperature.

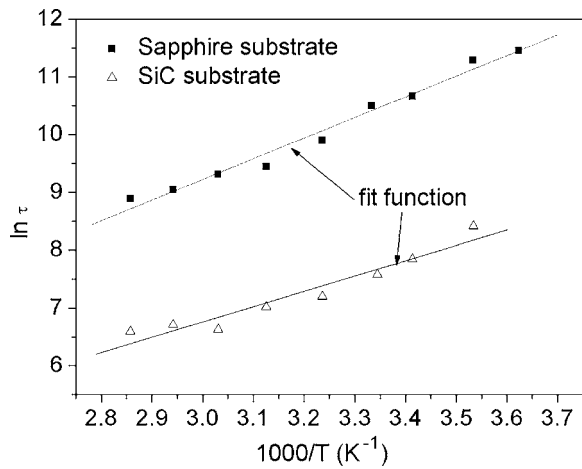


FIG. 8. Arrhenius plot of PPC decay time constant (τ vs $1000/T$) in the $\text{Al}_{0.20}\text{Ga}_{0.80}\text{N}/\text{GaN}/\text{sapphire}$ and $\text{Al}_{0.20}\text{Ga}_{0.80}\text{N}/\text{GaN}/\text{SiC}$ heterostructure samples.

The temperature dependence of PPC decay behavior was then fit to a well-known stretched-exponential function.

τ is dependent on temperature. This behavior can be explained as the probability of the thermal activation of the localized carriers to overcome the potential barrier increases by way of increasing temperature. The thermal carriers can escape to the recombination channels. The PPC decay rate, therefore, rapidly increases with increasing temperature. In the thermal activation region, this carrier capture barrier ΔE can be estimated from the temperature dependence of the time constant¹⁸

$$\tau = \tau_0 \exp[\Delta E/kT], \quad (2)$$

where τ_0 is the high temperature limit of the time constant and ΔE is the activation energy for the thermal capture of an electron at DX-like deep levels. Figure 8 shows the Arrhenius plot of τ with temperature. The resulting energy barriers for the capture of electrons in the 2DEG channel by the deep-level impurities (DX-like centers) in AlGaN for the $\text{Al}_{0.20}\text{Ga}_{0.80}\text{N}/\text{GaN}/\text{sapphire}$ and $\text{Al}_{0.20}\text{Ga}_{0.80}\text{N}/\text{GaN}/\text{SiC}$ heterojunction samples are 343 and 228 meV, respectively. The obtained ΔE value for $\text{Al}_{0.20}\text{Ga}_{0.80}\text{N}/\text{GaN}/\text{SiC}$ is consistent with the previously reported values.³⁴ However, the obtained ΔE value for sample A is larger than that in sample B. This result can be explained by the depth of the localization in $\text{Al}_{0.20}\text{Ga}_{0.80}\text{N}$. The depth of the localization is deeper for sample A. The different ranges of localization can be attributed to the effect of the larger cluster size in sample A.²⁵

IV. CONCLUSIONS

We studied the substrate material effects on the electrical and optical properties in $\text{Al}_x\text{Ga}_{1-x}\text{N}/\text{GaN}$ heterostructures ($x=0.20$). The illumination of the samples with a blue ($\lambda=470$ nm) LED induced a persistent increase in the carrier density and 2DEG electron mobility. In agreement with the previously reported PPC results, the PPC effect resulted in an increase in carrier and mobility density. In sample A, the carrier density increased from 7.59×10^{12} to 9.93×10^{12} cm^{-2} by illumination at 30 K. On the other hand, in

sample B, the increments in carrier density are larger than those in sample A and it increased from 7.62×10^{12} to 1.23×10^{13} cm^{-2} at the same temperature. This difference between the increment ratio comes from the DX density difference in the AlGa_xN layer as a result of the substrate type. The 2DEG mobility increased from 1.22×10^4 to 1.37×10^4 cm^2/Vs for samples A and B, and the 2DEG mobility increments occurred from 3.83×10^3 to 5.47×10^3 cm^2/Vs at 30 K. The PL results show that the samples exhibited a strong near-band-edge exciton luminescence line around 3.44 and 3.43 eV for samples A and B, respectively, and showed broad YB spreading from 1.80 to 2.60 eV with a peak maximum at 2.25 eV, wherein the ratio of the near-band-edge excitation peak intensity to the deep-level emission peak intensity ratio was equal to 3 and 1.8 for samples $\text{Al}_{0.20}\text{Ga}_{0.80}\text{N}/\text{GaN}/\text{sapphire}$ and $\text{Al}_{0.20}\text{Ga}_{0.80}\text{N}/\text{GaN}/\text{SiC}$, respectively. Both of the samples were illuminated with three different energy photons. We observed different decay rates for three different photon energy levels. These behaviors can usually be attributed to the presence of carrier localization states and are explained based on the alloy compositional fluctuations in the $\text{Al}_x\text{Ga}_{1-x}\text{N}$ alloys. The PPC decay behavior can be well described by a stretched-exponential function and the relaxation time constant τ , in which the decay exponent β changes with the substrate material. The energy barriers for the capture of electrons in the 2DEG channel by the deep-level impurities (DX-like centers) in AlGa_xN for the $\text{Al}_{0.20}\text{Ga}_{0.80}\text{N}/\text{GaN}/\text{sapphire}$ and $\text{Al}_{0.20}\text{Ga}_{0.80}\text{N}/\text{GaN}/\text{SiC}$ heterojunction samples are 343 and 228 meV, respectively. The activation energy for the thermal capture of an electron by defects ΔE was found to change with the substrate materials. Our results have revealed that the substrate material strongly affects the electrical and optical properties of $\text{Al}_{0.20}\text{Ga}_{0.80}\text{N}/\text{GaN}$ heterostructures. These results can be explained with the differing degrees of lattice mismatch between the grown layers and substrates.

ACKNOWLEDGMENTS

This work was supported by the European Union under the Project Nos. EU-NoE-METAMORPHOSE and EU-NoE-PHOREMOST and TUBITAK under the Project Nos. 105E066, 105A005, 106E198, and 106A017. One of the authors (E.O.) also acknowledges partial support from the Turkish Academy of Sciences.

¹S. N. Mohammad, A. Salvador, and H. Morkoç, Proc. IEEE **83**, 1420 (1996).

²L. Shen, S. Heikman, B. Moran, R. Coffie, N.-Q. Zhang, D. Buttari, I. P. Smorchkova, S. Keller, S. P. DenBaars, and U. K. Mishra, IEEE Electron Device Lett. **22**, 457 (2001).

³S. Butun, M. Gokkavas, H. Yu, and E. Ozbay, Appl. Phys. Lett. **89**, 073503 (2006).

⁴T. Tut, M. Gokkavas, B. Butun, S. Butun, E. Ulker, and E. Ozbay, Appl. Phys. Lett. **89**, 183524 (2006).

⁵S. Nakamura, M. Senoh, S. Nagahama, N. Iwasa, T. Yamada, T. H. Kiyoku, Y. Sugimoto, T. Kozaki, H. Umemoto, M. Sano, and K. Chocho, Appl. Phys. Lett. **72**, 1687 (1998).

⁶A. Y. Polyakov, N. B. Smirnov, A. S. Usikov, A. V. Govorkov, and B. V. Pushniy, Solid-State Electron. **42**, 627 (1998).

⁷L. Hsu and W. Walukiewicz, Phys. Rev. B **56**, 1520 (1997).

⁸T. Wang, Y. Ohno, M. Lacha, D. Nakagawa, T. Shirahama, S. Sakai, and H. Ohno, Appl. Phys. Lett. **74**, 3531 (1999).

- ⁹M. Redwing, M. A. Tischler, J. S. Flynn, S. Elhamri, M. Ahoujja, and R. S. W. C. Mitchel, *Appl. Phys. Lett.* **69**, 963 (1996).
- ¹⁰N. Biyikli, Ü. Özgür, X. Ni, Y. Fu, H. Morkoç, and Ç. Kurdak, *J. Appl. Phys.* **100**, 103702 (2006).
- ¹¹H. Yu, D. Caliskan, and E. Ozbay, *J. Appl. Phys.* **100**, 033501 (2006).
- ¹²R. Gaska, J. W. Yang, A. Osinsky, Q. Chen, M. Asif Khan, A. O. Orlov, G. L. Snider, and M. S. Shur, *Appl. Phys. Lett.* **72**, 707 (1998).
- ¹³A. Dadgar, C. Hums, A. Diez, J. Bläsing, and A. Krost, *J. Cryst. Growth* **297**, 279 (2006).
- ¹⁴X. Z. Dang, C. D. Wang, E. T. Yu, K. S. Boutros, and J. M. Redwing, *Appl. Phys. Lett.* **72**, 2745 (1998).
- ¹⁵C. H. Qiu, C. Hoggatt, W. Melton, M. W. Leksono, and J. I. Pankove, *Appl. Phys. Lett.* **66**, 2712 (1995).
- ¹⁶H. X. Jiang and J. Y. Lin, *Phys. Rev. B* **40**, 10025 (1989).
- ¹⁷D. V. Lang, R. A. Logan, and M. Joros, *Phys. Rev. B* **19**, 1015 (1979).
- ¹⁸H. J. Queisser and D. E. Theodorou, *Phys. Rev. B* **33**, 4027 (1986).
- ¹⁹N. Sarkar, S. Dhar, and S. Ghosh, *J. Phys.: Condens. Matter* **15**, 7325 (2003).
- ²⁰M. A. Reshchikov, G.-C. Yi, and B. W. Wessels, *Phys. Rev. B* **59**, 13176 (1999).
- ²¹J. Z. Li, J. Y. Lin, H. X. Jiang, A. Salvador, A. Botchkarev, and H. Morkoc, *Appl. Phys. Lett.* **69**, 1474 (1996).
- ²²S. J. Chung, B. Karunakaran, S. Velumani, C.-H. Hong, H. J. Lee, and E.-K. Suh, *Appl. Phys. A: Mater. Sci. Process.* **86**, 521 (2007).
- ²³X. Z. Dang, C. D. Wang, E. T. Yu, K. S. Boutros, and J. M. Redwing, *Appl. Phys. Lett.* **72**, 2745 (1998).
- ²⁴J. Z. Li, J. Y. Lin, H. X. Jiang, M. Asif Khan, and Q. Chen, *J. Appl. Phys.* **82**, 1227 (1997).
- ²⁵S. J. Chung, M. Senthil Kumar, H. J. Lee, and E.-K. Suh, *J. Appl. Phys.* **95**, 3565 (2004).
- ²⁶K. C. Zeng, J. Y. Lin, and H. X. Jiang, *Appl. Phys. Lett.* **76**, 1728 (2000).
- ²⁷A. Dissanayake, M. Elahi, H. X. Jiang, and J. Y. Lin, *Phys. Rev. B* **45**, 13996 (1992).
- ²⁸K. C. Zeng, J. Y. Lin, and H. X. Jiang, *Appl. Phys. Lett.* **76**, 1728 (2000).
- ²⁹Z. Peng, T. Saku, and Y. Horikoshi, *J. Appl. Phys.* **79**, 3592 (1996).
- ³⁰T. Y. Lin, H. M. Chen, M. S. Tsai, Y. F. Chen, F. F. Fang, C. F. Lin, and G. C. Chi, *Phys. Rev. B* **58**, 13793 (1998).
- ³¹H. M. Chen, Y. F. Chen, M. C. Lee, and M. S. Feng, *J. Appl. Phys.* **82**, 899 (1997).
- ³²S. J. Chung, M. Senthil Kumar, Y. K. Kim, C.-H. Hong, H. J. Lee, and E.-K. Suh, *J. Korean Phys. Soc.* **45**, 1279 (2004).
- ³³C. Wetzel, T. Suski, J. W. Ager, E. R. Weber, S. Fischer, B. K. Meyer, R. J. Molnar, and P. Perlin, *Phys. Rev. Lett.* **78**, 3923 (1997).
- ³⁴J. Z. Li, J. Y. Lin, H. X. Jiang, M. A. Khan, and Q. Chen, *J. Vac. Sci. Technol. B* **15**, 1117 (1997).
- ³⁵M. N. Gurusinge, S. K. Davidsson, and T. G. Andersson, *Phys. Rev. B* **72**, 045316 (2005).
- ³⁶J. Antoszewski, M. Gracey, J. M. Dell, L. Faraone, T. A. Fisher, G. Parish, Y.-F. Wu, and U. K. Mishra, *J. Appl. Phys.* **87**, 3900 (2000).
- ³⁷S. J. Chung, O. H. Cha, Y. S. Kim, M. S. Jeong, C.-H. Hong, H. J. Lee, M. S. Jeong, J. O. White, and E.-K. Suh, *J. Appl. Phys.* **89**, 5454 (2001).
- ³⁸T. Y. Lin, H. C. Yang, and Y. F. Chen, *J. Appl. Phys.* **87**, 3404 (2000).
- ³⁹C. H. Qiu and J. I. Pankove, *Appl. Phys. Lett.* **70**, 1983 (1997).
- ⁴⁰L. H. Chu, Y. F. Chen, D. C. Chang, and C. Y. Chang, *J. Phys.: Condens. Matter* **7**, 4525 (1995).
- ⁴¹C. Johnson, J. Y. Lin, H. X. Jiang, M. A. Khan, and C. J. Sun, *Appl. Phys. Lett.* **68**, 1808 (1996).